American Journal of Case Reports

e-ISSN 1941-5923
© Am J Case Rep, 2026; 27: e953906
DOI: 10.12659/AJCR.953906

Received: 2026.04.25
Accepted: 2026.10.13
Available online: 2026.10.26
Published: 2026.XX.XX

Systemic Amyloid Light-Chain Amyloidosis Associated With Multiple Myeloma in a Young Adult With Multisystem Complications: Ischemic Stroke, Bilateral Scleromalacia Perforans, and Intestinal Perforation

Authors' Contribution:
Study Design A
Data Collection B
Statistical Analysis C
Data Interpretation D
Manuscript Preparation E
Literature Search F
Funds Collection G

ABDEF 1,2 Angelica Mandujano
DEF 1 Mario Mandujano
DEF 3 Melissa Golubov
BDEF 2 Carlos Alberto Reyes-Gómez

1 Department of Health Care, Universidad Autónoma Metropolitana-Xochimilco, México City, México
2 Department of Internal Medicine, Hospital San Ángel Inn, Universidad, México City, México
3 Department of Immunology, Facultad de Medicina, Universidad Nacional Autónoma de México, México City, México

Corresponding Author: Angelica Mandujano, Calzada del Hueso 1100, Coapa, Villa Quietud, Coyoacán, 04960, México City, México
Phone: +525520825127, e-mail: amandujano@correo.xoc.uam.mx

Financial support: None declared
Conflict of interest: None declared

Patient: Male, 41-year-old
Final Diagnosis: AL amyloidosis associated with multiple myeloma
Symptoms: Anasarca • constitutional symptoms • dyspnea • hoarseness • inflammatory low back pain • inflammatory polyarthralgia • neurological deficit
Clinical Procedure: —
Specialty: Cardiology • Hematology • Neurology • Rheumatology
Objective: Unusual clinical course

Background: Amyloid light-chain amyloidosis is the most common form of systemic amyloidosis; however, it remains a rare disease. It is most often associated with non-malignant plasma cell dyscrasias but may also occur with multiple myeloma. Both conditions predominantly affect older adults. We report an unusual case of amyloid light-chain amyloidosis associated with multiple myeloma in a middle-aged adult, to highlight the diagnostic challenge posed by delayed recognition followed by severe multisystem complications.

Case Report: A 41-year-old man presented with a 4-year history of constitutional symptoms, inflammatory arthralgias, bilateral carpal tunnel syndrome, nephrotic-range proteinuria, and progressive multisystem involvement. Initial immunologic and infectious investigations were negative. Systemic amyloidosis was suspected, but the patient was lost to follow-up. Reassessment demonstrated monoclonal lambda free light chains and multiple characteristic echocardiographic findings suggestive of cardiac amyloidosis. Before hematologic evaluation was completed, he developed an acute ischemic stroke followed by cardiac arrest. During hospitalization, he developed bilateral scleromalacia perforans and, days later, upper gastrointestinal perforation complicated by septic shock, leading to death. Congo red-positive minor salivary gland biopsy findings, together with bone marrow biopsy demonstrating lambda-restricted plasma cell infiltration, monoclonal protein studies, and multiple osteolytic lesions, established the diagnosis of systemic amyloid light-chain amyloidosis associated with multiple myeloma.

Conclusions: This case highlights the importance of considering amyloid light-chain amyloidosis and plasma cell disorders in middle-aged adults with nephrotic-range proteinuria and multisystem infiltrative features despite an atypical age at presentation. Although a single case cannot establish causality, delayed recognition may be followed by severe, potentially life-threatening complications in advanced multisystem disease.

Keywords: Amyloidosis • Intestinal Perforation • Multiple Myeloma • Scleritis • Stroke
Full-text PDF: https://www.amjcaserep.com/abstract/index/idArt/953906

3794 1 8 44

Publisher's note: All claims expressed in this article are solely those of the authors and do not necessarily represent those of their affiliated organizations, or those of the publisher, the editors and the reviewers. Any product that may be evaluated in this article, or claim that may be made by its manufacturer, is not guaranteed or endorsed by the publisher

APPROVED GALLEY PROOF

This work is licensed under Creative Commons Attribution-NonCommercial-NoDerivatives 4.0 International (CC BY-NC-ND 4.0)

Indexed in: [PMC] [PubMed] [Emerging Sources Citation Index (ESCI)] [Web of Science by Clarivate]

APPROVED GALLEY PROOF

Introduction

Amyloidosis is a group of disorders characterized by extracellular deposition of amyloid fibrils in organs [1]. Forty-two precursor amyloidogenic human proteins have been identified [2]. Amyloid light-chain (AL) amyloidosis is characterized by deposition of fibril-forming monoclonal kappa or lambda light chains in tissues, leading to progressive organ dysfunction. AL amyloidosis is most commonly associated with clonal plasma cell dyscrasias but may also occur in patients with multiple myeloma (MM). Although virtually any organ can be involved, the heart and kidneys are most frequently affected [1,3]. A global systematic review estimated a prevalence of approximately 50 cases per million and an incidence of 10 cases per million person-years [3]. Despite advances in diagnosis and treatment, prognosis remains poor, particularly in patients with cardiac amyloidosis (CA) and multiorgan involvement [4,5].

AL amyloidosis and MM predominantly affect older adults. The mean age at diagnosis of AL amyloidosis is approximately 60 years, while MM has a median age at diagnosis of 69 years; only 2.6% of cases occur between 35 and 44 years of age [4,6,7]. The reported prevalence of clinically overt AL amyloidosis among patients with MM ranges from 7% to 15%, while Congo red-positive amyloid deposits without clinically apparent amyloidosis have been reported in approximately a third of patients undergoing fat pad biopsy [6,8,9]. Together, these epidemiologic observations provide the context for the unusual presentation described in this report.

The present case illustrates the diagnostic challenge of systemic AL amyloidosis associated with MM in a middle-aged adult, with initially nonspecific manifestations contributing to delayed recognition. It also highlights an unusual constellation of severe complications, including ischemic stroke, bilateral scleromalacia perforans, and upper gastrointestinal perforation. We report this case to emphasize that AL amyloidosis associated with MM should remain in the differential diagnosis of patients presenting with nephrotic-range proteinuria and multisystem infiltrative features, even in those outside the typical age range, as earlier recognition may allow consideration of disease-directed therapy before advanced organ dysfunction develops.

Case Report

A 41-year-old Hispanic man with hoarseness was evaluated by an otorhinolaryngologist. Laryngoscopy was not feasible because of tongue and hypopharyngeal enlargement. He was subsequently referred to an oral pathologist because of oral burning, xerostomia, and recurrent oral ulcers. A minor salivary gland (lip) biopsy was performed (**Figure 1**). He was also referred to a rheumatologist, given the systemic and musculoskeletal manifestations. The patient was first assessed at the Rheumatology Service in early October. His past medical history included smoking, alcohol consumption, recreational drug use, and a history of 10 unprotected sexual contacts. He had undergone surgery for bilateral carpal tunnel syndrome. During the preceding 4 years, he had experienced inflammatory lower back and heel pain, as well as large joint inflammatory arthralgia (shoulders and hips) accompanied by prolonged morning stiffness. Over the following year, his disease progressed from predominantly musculoskeletal symptoms to multisystem involvement. These included progressive edema evolving to anasarca, constitutional symptoms (malaise, severe

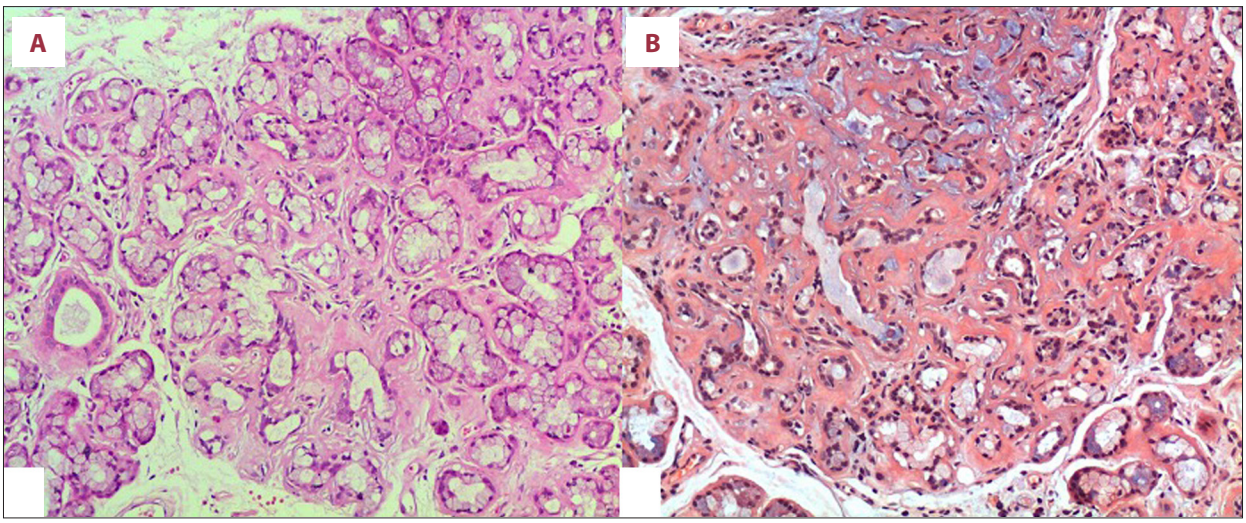


Figure 1. Lower lip minor salivary gland biopsy. (**A**) Amorphous eosinophilic material with periductal and periacinar distribution is present in the minor salivary glands on hematoxylin and eosin staining (H&E, 100 ×). (**B**) Congo red staining demonstrates amyloid deposits (100 ×).

This work is licensed under Creative Commons Attribution-NonCommercial-NoDerivatives 4.0 International (CC BY-NC-ND 4.0)

Indexed in: [PMC] [PubMed] [Emerging Sources Citation Index (ESCI)] [Web of Science by Clarivate]

Table 1. Laboratory investigations performed during the diagnostic workup. Results are presented according to the initial clinical suspicion and the main differential diagnoses.

Category	Parameters	Result	Comments
Complete blood cell count	White blood cells	5.5 × 10^9/L	Normal
	Hemoglobin	14.1 g/dL	Normal
	Platelet count	270 × 10^9/L	Normal
Serum chemistry	Glucose	95 mg/dL	Normal
	Blood urea nitrogen	25 mg/dL	Normal
	Creatinine	2.2 mg/dL	Elevated
	Albumin	3.9 g/dL	Normal
Serum electrolytes	Sodium	138 mEq/L	Normal
	Potassium	4.4 mEq/L	Normal
	Calcium	9.7 mg/dL	Normal
Urinalysis	Spot urine protein/creatinine ratio	5740 mg/g	Elevated (nephrotic range)
	Urinary sediment	3+ proteins, 2+ hemoglobin, absent casts, 3-10 erythrocytes/field	Abnormal
	Urine culture	Negative	
Serum immunoglobulins	IgG	4.67 g/L	Low
	IgA	< 0.268 g/L	Low
	IgM	< 0.192 g/L	Low
Complement	C3	130 mg/dL	Normal
	C4	49 mg/dL	Normal
Autoantibodies	ANA	1: 160	Cytoplasmatic pattern
	dsDNA, ANCA, RF, ACPA, HLA-B27, HIV	Negative	
Acute phase reactants	C-reactive protein	6.77 mg/L	Elevated
	Thyroid and liver function tests	Normal	

ANA, antinuclear antibody; dsDNA, double-stranded DNA; ANCA, anti-neutrophil cytoplasmic antibodies; RF, rheumatoid factor; ACPA, anti-citrullinated protein antibodies; HLA, human leukocyte antigen; HIV, Human Immunodeficiency Virus.

fatigue, weakness, anorexia, and a 4-6 kg weight loss), exertional dyspnea, persistent oral manifestations (dysphagia), and gastrointestinal symptoms including abdominal bloating, severe constipation, and hemorrhoids. Physical examination revealed mild pitting edema, inflammatory low back pain, and shoulder and hip arthralgia with no clinical evidence of synovitis nor enthesitis.

At this initial rheumatologic evaluation, the patient presented with laboratory results obtained in August, including a complete blood count, blood chemistry panel, and C-reactive protein (CRP), all of which were within normal limits. Initially, an autoimmune connective tissue disease, particularly systemic lupus erythematosus, was suspected based on the patient´s prolonged clinical course, systemic manifestations, and epidemiological factors. Other diagnostic considerations included systemic vasculitis, spondyloarthritis, and human immunodeficiency virus (HIV) infection. However, laboratory test results were not consistent with these diagnoses. The initial diagnostic workup is summarized in **Table 1**.

Amyloidosis was also considered as a possible diagnosis, prompting further diagnostic evaluation and referral to Nephrology. However, the patient was lost to follow-up.

APPROVED GALLEY PROOF

This work is licensed under Creative Commons Attribution-NonCommercial-NoDerivatives 4.0 International (CC BY-NC-ND 4.0)

Indexed in: [PMC] [PubMed] [Emerging Sources Citation Index (ESCI)] [Web of Science by Clarivate]

APPROVED GALLEY PROOF

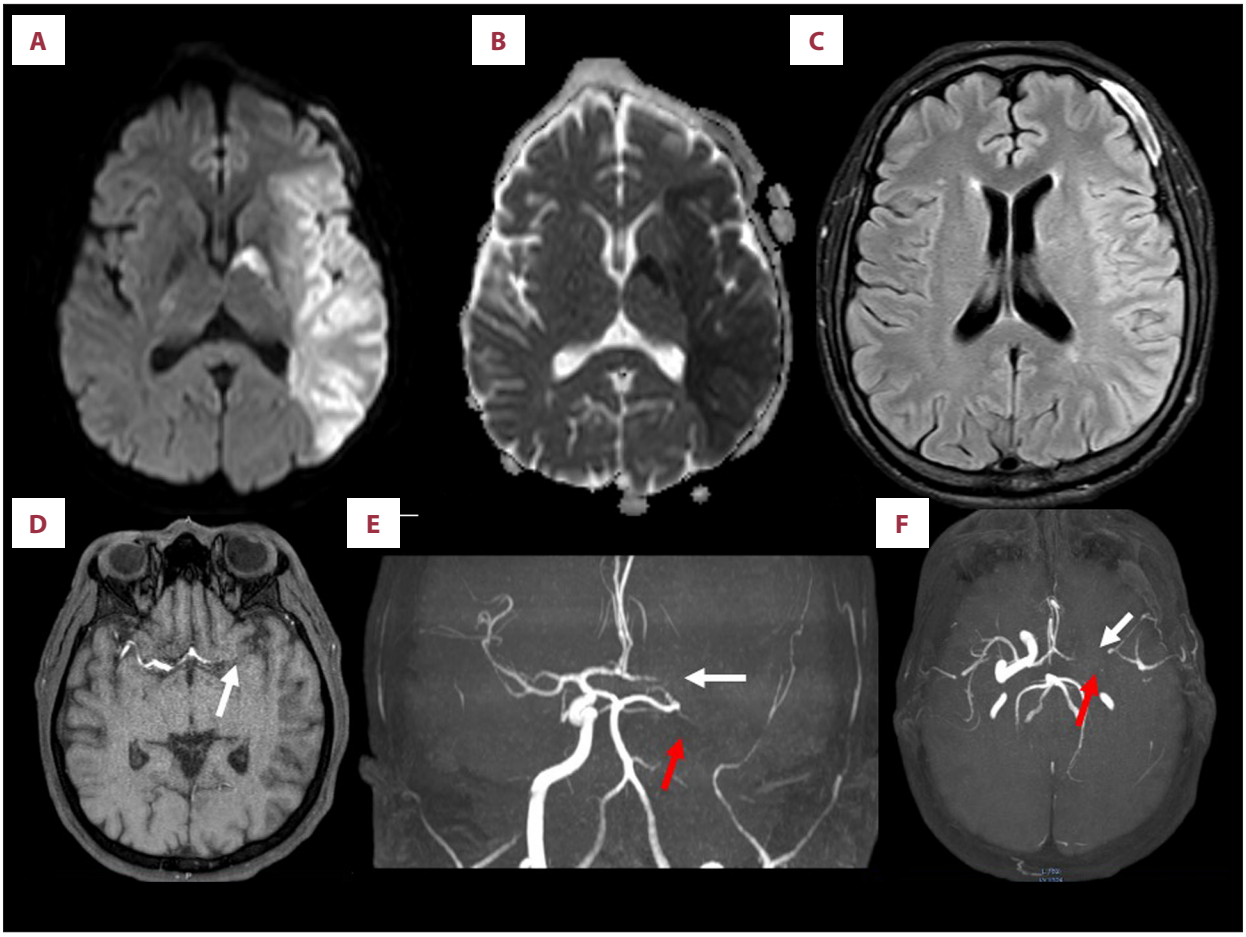


Figure 2. (**A, B**) Axial diffusion-weighted magnetic resonance imaging of the brain demonstrates a hyperintense area consistent with restricted diffusion, with corresponding low signal on the apparent diffusion coefficient map, indicating an acute infarct in the territory of the left middle cerebral artery (ASPECTS 3/10). (**C**) T2-weighted fluid-attenuated inversion recovery (FLAIR) images show cortico-subcortical hyperintensity involving the left temporoparietal and insular regions, with an associated calvarial lytic lesion. (**D**) Axial 3D time-of-flight (TOF) magnetic resonance angiography demonstrates loss of flow-related signal in the M1 segment of the left middle cerebral artery (white arrows). (**E, F**) Coronal TOF images demonstrate loss of flow-related signal in the left internal carotid artery on maximum intensity projection images, consistent with occlusion of the left internal carotid artery (red arrows), with an abrupt cutoff of the left middle cerebral artery at the M1 segment (white arrows).

Three months later, the patient returned to follow-up due to worsening of his general condition, with an increase in constitutional, musculoskeletal, and gastrointestinal symptoms. Upon resuming follow-up, laboratory tests showed a monoclonal spike in serum protein electrophoresis. Serum immunofixation identified monoclonal lambda light chains, and a 24-hour urine immunofixation demonstrated presence of total and free monoclonal lambda light chains. Serum free light chain analysis showed a kappa chain level of 11.8 mg/L and a lambda chain level of 4850 mg/L, yielding a free light chain ratio (involved/uninvolved) of 411. Transthoracic echocardiography demonstrated concentric left ventricular wall thickening (interventricular septum 14 mm; posterior wall 12 mm), preserved left ventricular ejection fraction, grade II diastolic dysfunction with elevated filling pressures (E/e' ratio 24), thickening of the atrioventricular and semilunar valves, biatrial dilatation, and impaired right ventricular systolic function (TAPSE 10 mm). Speckle-tracking echocardiography revealed markedly reduced global longitudinal strain (-11.7%) with relative apical sparing. Altogether, these findings were highly suggestive of CA. He was referred to Hematology for a bone marrow biopsy.

Before the hematology evaluation could be completed, he was admitted to the emergency department, following acute neurological deterioration. Family members reported that he had fallen out of bed at dawn, sustaining a mild contusion on the left frontal region without loss of consciousness. He returned to bed but was found the next morning disoriented, with generalized weakness and difficulty staying upright. On

This work is licensed under Creative Commons Attribution-NonCommercial-NoDerivatives 4.0 International (CC BY-NC-ND 4.0)

Indexed in: [PMC] [PubMed] [Emerging Sources Citation Index (ESCI)] [Web of Science by Clarivate]

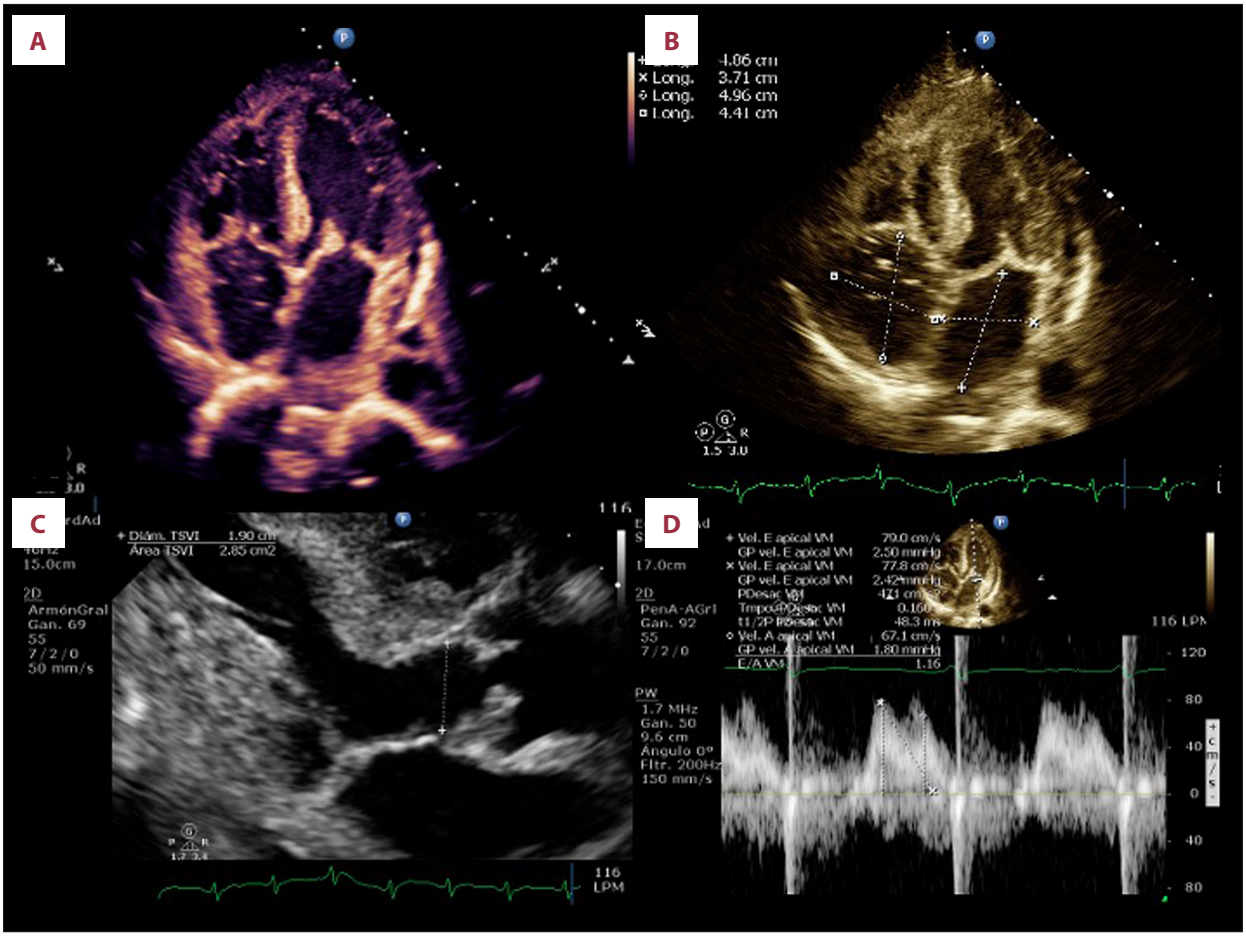


Figure 3. Transthoracic echocardiographic findings. (**A**) Two-dimensional echocardiography demonstrates biventricular hypertrophy, a granular sparkling appearance of the myocardium, and thickening of the cardiac valves. (**B**) Apical 4-chamber view reveals biatrial enlargement. (**C**) Left parasternal long-axis view shows concentric left ventricular hypertrophy with a sparkling appearance of the myocardium. (**D**) Pulsed wave Doppler assessment of mitral inflow demonstrates a pseudonormal transmitral filling pattern consistent with grade II left ventricular diastolic dysfunction. Left ventricular ejection fraction was preserved.

admission, the Glasgow Coma Scale score was 14/15 (E: 4, V: 4, M: 6). The patient was cooperative and able to obey simple commands but experienced mild somnolence, disorientation, and generalized weakness, without focal neurological deficits or external signs of trauma. The most relevant laboratory findings were a creatinine level of 1.29 mg/dL, sodium of 128 mmol/L, N-terminal pro-B-type natriuretic peptide (NT-proBNP) of 3579 pg/mL, and troponin I of 0.5 ng/mL. He was started on hypertonic saline for moderate hyponatremia and was admitted for further evaluation of suspected AL amyloidosis. Within 24 hours, he developed right upper limb monoplegia, right lower limb paresis, and mild left oral commissure deviation. Brain magnetic resonance imaging (MRI) documented an acute ischemic stroke in the left middle cerebral artery associated with left internal carotid artery occlusion, suggestive of artery-to-artery embolism (**Figure 2**). The neurological deficits progressed to right hemiplegia and aphasia, requiring admission to the intensive care unit. Cardiology confirmed CA based on elevated cardiac biomarkers and echocardiographic findings (**Figure 3**). Based on the initial NT-proBNP, cardiac troponin I, and difference in free light chain (dFLC) values, the patient fulfilled Revised Mayo 2012 stage IIIa criteria [10].

Therapeutic anticoagulation with enoxaparin was initiated after multidisciplinary evaluation because of the patient's high thromboembolic risk. At the time anticoagulation was started, there was no clinical evidence of bleeding diathesis, spontaneous mucocutaneous bleeding or the characteristic periorbital purpura described in AL amyloidosis. Anticoagulation was well tolerated. Two days later, neurological and respiratory status worsened, requiring orotracheal intubation and mechanical ventilation. He developed hemodynamic decompensation and pulseless electrical activity that required advanced resuscitation, with favorable response.

APPROVED GALLEY PROOF

This work is licensed under Creative Commons Attribution-NonCommercial-NoDerivatives 4.0 International (CC BY-NC-ND 4.0)

Indexed in: [PMC] [PubMed] [Emerging Sources Citation Index (ESCI)] [Web of Science by Clarivate]

APPROVED GALLEY PROOF

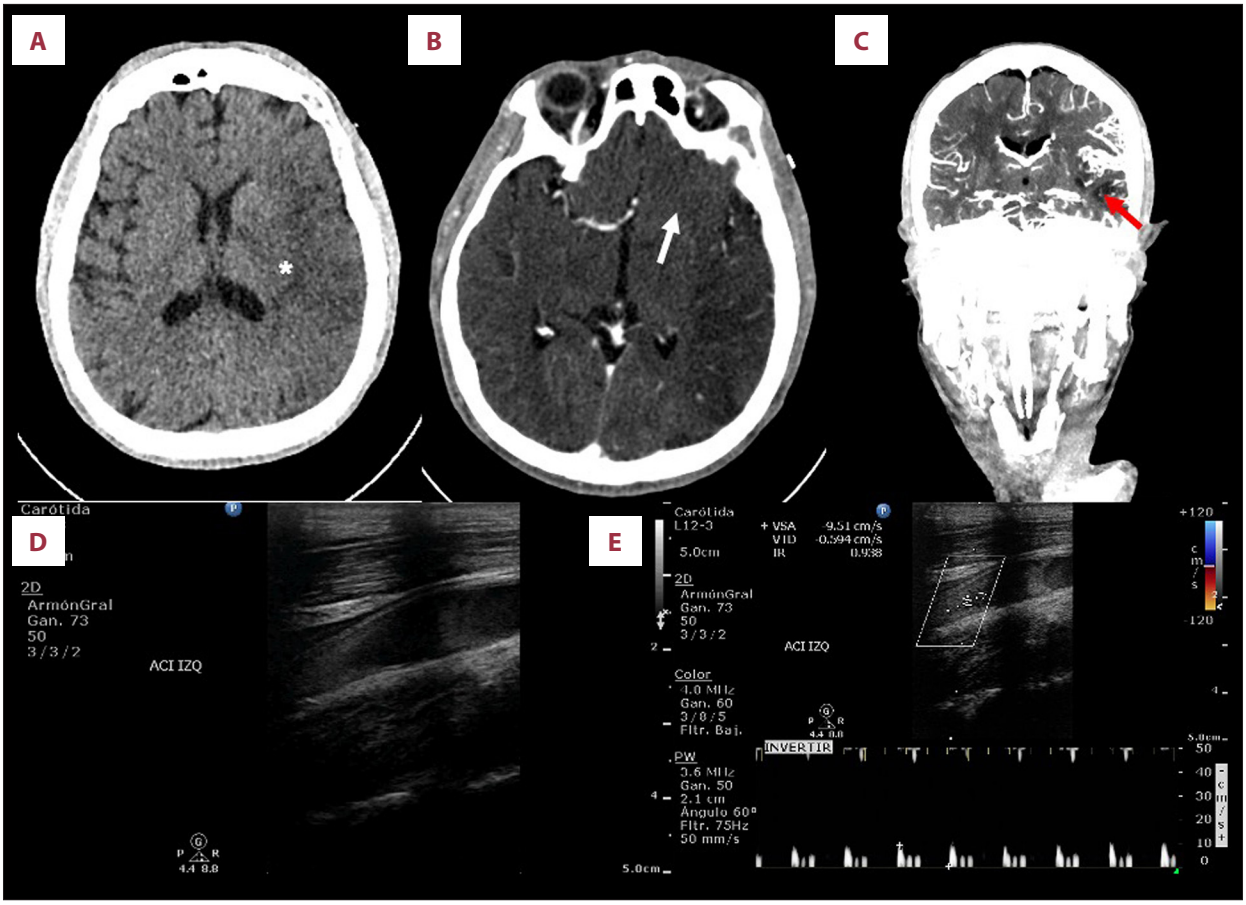


Figure 4. Neurovascular imaging findings. (**A-C**) Axial computed tomography (CT) images demonstrate findings consistent with acute ischemic stroke in the territory of the left middle cerebral artery. Cerebral edema with effacement of cortical sulci and fissures is observed at the left temporoparietal and insular regions, accompanied by cortical and subcortical hypodensity and loss of gray-white matter differentiation. (**A**) Hypodensity involving the left basal ganglia and posterior limb of the internal capsule is also observed (white asterisk). (**B**) CT angiography demonstrates occlusion of the M1 segment of the left middle cerebral artery (white arrow, axial view). (**C**) Coronal angiographic reconstruction demonstrates partial recanalization with residual narrowing of the M2 segment (red arrow) and increased cortical vascularity. (**D**) B-mode ultrasound demonstrates an intraluminal echogenic image at the left carotid bulb suggestive of thrombus. (**E**) Color Doppler demonstrates no detectable color flow signal within the left internal carotid artery. Spectral Doppler of the ipsilateral common carotid artery, obtained proximal to the occlusion, demonstrates a high-resistance waveform with absent diastolic flow.

Computed tomography (CT) angiography and carotid ultrasound were performed (**Figure 4**). A bone marrow biopsy was also obtained (**Figure 5**). Although renal biopsy was considered during the nephrological evaluation, it was not ultimately performed because diagnostic tissue had already been obtained from the minor salivary gland and bone marrow, and additional renal tissue was unlikely to alter subsequent patient management. Formal renal staging was not applied because the available 24-hour urine collection was obtained after substantial deterioration in renal function and was considered unlikely to accurately reflect the severity of renal involvement at presentation. Five days after admission, the patient developed a scleral lesion. Ophthalmologic evaluation was consistent with bilateral scleromalacia perforans, a non-inflammatory form of necrotizing scleritis (**Figure 6**). Given the severity of ocular involvement and the risk of progressive scleral destruction, corticosteroid therapy was initiated with intravenous methylprednisolone pulses (1 g daily for 3 consecutive days), followed by oral prednisone (50 mg/day) [11,12]. Alternative causes were investigated. Venereal Disease Research Laboratory testing, HIV serology, and GeneXpert *Mycobacterium tuberculosis* (MTB) testing were negative. Repeated antinuclear antibodies (ANA), anti-neutrophil cytoplasmic antibodies (ANCA), anti-myeloperoxidase (anti-MPO), and anti-proteinase 3 (anti-PR3) antibodies were also negative. Rheumatoid factor and anti-citrullinated protein antibodies (ACPA) had been previously negative. Together, these findings supported the clinical diagnosis of bilateral scleromalacia perforans in the setting of systemic AL amyloidosis.

This work is licensed under Creative Commons Attribution-NonCommercial-NoDerivatives 4.0 International (CC BY-NC-ND 4.0)

Indexed in: [PMC] [PubMed] [Emerging Sources Citation Index (ESCI)] [Web of Science by Clarivate]

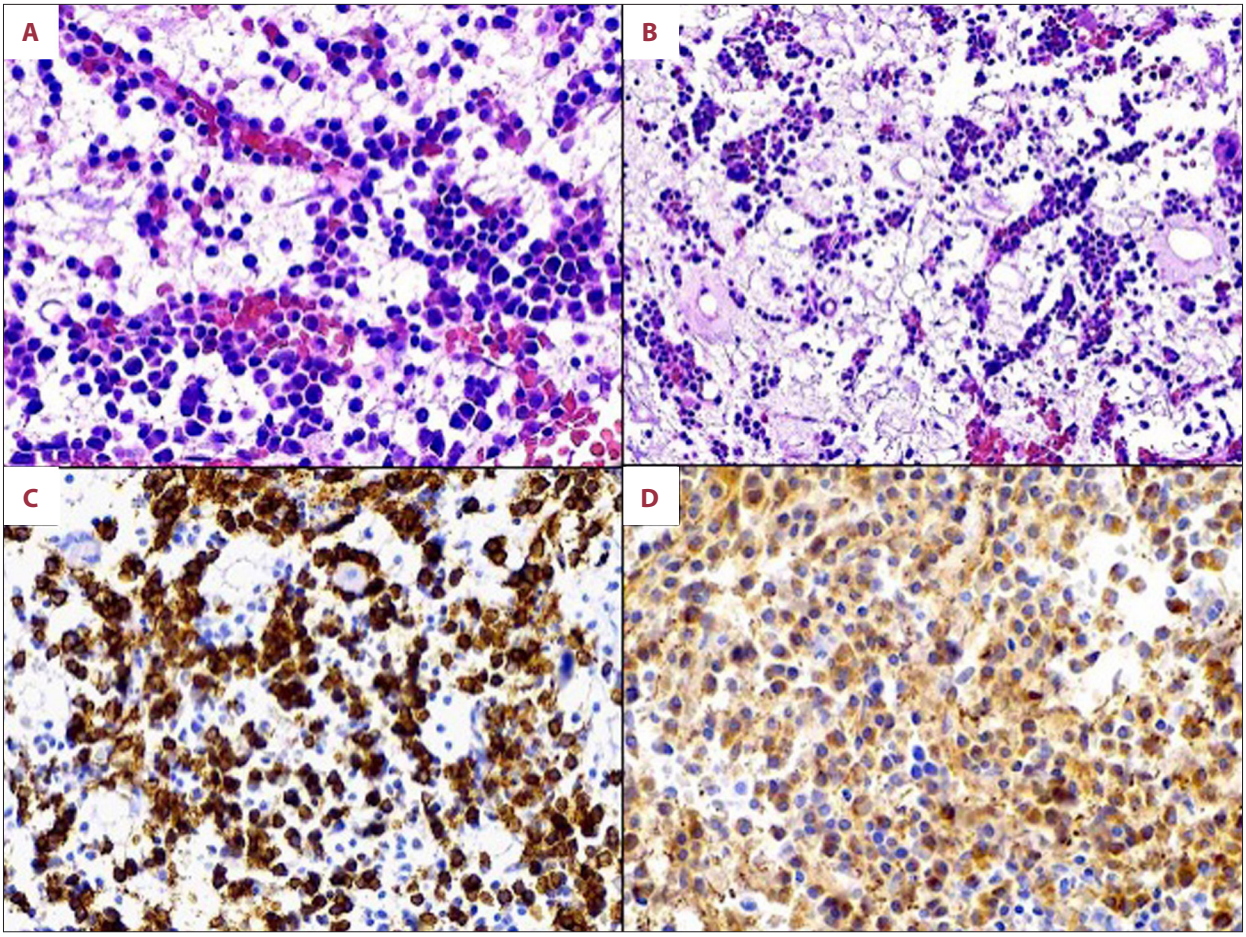


Figure 5. Bone marrow biopsy demonstrates a hypocellular marrow (overall cellularity 25%) with interstitial and diffuse infiltration of plasma cells, consistent with multiple myeloma with lambda light-chain restriction. (**A**) Mature plasma cells account for 70% of total cellularity, without evidence of myelofibrosis. (**B**) The interstitium shows myxoid stromal changes. Immunohistochemical staining (**C**) demonstrates strong CD138 positivity (3+) and MUM1 positivity (3+) in neoplastic plasma cells, with absence of kappa expression and strong lambda light-chain positivity (3+), demonstrating lambda light-chain restriction (**D**).

Ten days after admission, he developed abdominal distension, fever, and peritoneal signs. An abdominal ultrasound demonstrated portal vein gas. Subsequent CT confirmed this finding (**Figure 7**) and demonstrated osteolytic bone lesions. Emergency surgical evaluation was performed; however, surgical intervention was considered prohibitively high risk because of advanced multisystem disease, severe cardiac involvement, recent ischemic stroke, previous cardiac arrest, hemodynamic instability, and evolving septic shock. After discussion of risks and prognosis, the family declined surgical intervention. Despite conservative medical treatment including supportive care, broad-spectrum antibiotics, and vasopressors, the patient developed refractory hypotension and progressive bradycardia. He ultimately died from septic shock 13 days after admission.

The diagnosis of systemic AL (λ) amyloidosis was established through the integration of histopathologic, hematologic, laboratory, and clinical findings. Amyloid deposition was confirmed by Congo red staining of a minor salivary gland biopsy. Bone marrow biopsy demonstrated 70% infiltration of mature neoplastic plasma cells expressing CD138 (3+) and MUM1/IRF4 (3+), with immunohistochemical evidence of λ light-chain restriction, confirming a monoclonal λ-producing plasma cell population. Serum protein electrophoresis, serum immunofixation, and 24-hour urine immunofixation identified a monoclonal protein, while serum free light chain analysis revealed markedly elevated λ free light chains with an involved/uninvolved free light chain ratio (λ/κ) of 411. The diagnosis of symptomatic MM was further supported by multiple osteolytic lesions involving the skull, spine, and sacrum. The patient also had nephrotic-range proteinuria, CA, and findings suggestive of gastrointestinal involvement, all consistent with systemic AL amyloidosis. Although direct amyloid typing by laser microdissection and mass spectrometry was not available, the combination of

APPROVED GALLEY PROOF

This work is licensed under Creative Commons Attribution-NonCommercial-NoDerivatives 4.0 International (CC BY-NC-ND 4.0)

Indexed in: [PMC] [PubMed] [Emerging Sources Citation Index (ESCI)] [Web of Science by Clarivate]

APPROVED GALLEY PROOF

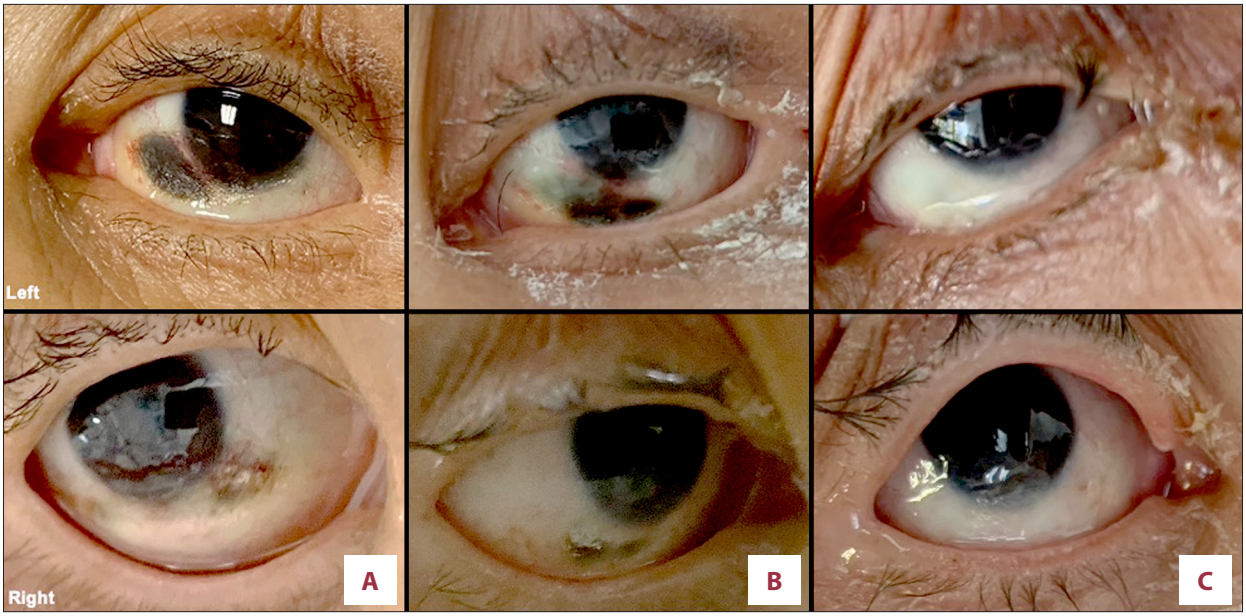


Figure 6. Bilateral scleral involvement and therapeutic response. A 10 × 3 mm area of scleral thinning extending to the inferior nasal portion of the sclerocorneal limbus of the left eye was observed. Twenty-four hours later, a similar lesion developed in the right eye. Panel **A** shows bilateral scleral lesions before treatment; Panel **B** demonstrates the lesions during therapy. Panel **C** shows marked clinical improvement with resolution of the visible scleral lesions in both eyes after completion of the third intravenous methylprednisolone pulse.

Congo red-positive tissue deposits, a λ-restricted plasma cell neoplasm with marked monoclonal λ light-chain production, and typical multisystem organ involvement supported the diagnosis of systemic AL (λ) amyloidosis. **Figure 8** presents a timeline summarizing the most relevant features of the case.

Discussion

To contextualize the diagnostic warning message of this case, we review available literature on each of the 3 complications that followed diagnostic delay in our patient. Few case reports have described ischemic stroke in the setting of AL amyloidosis [13-15]. Zubkov et al conducted a retrospective study of 40 patients with amyloidosis and stroke. In their cohort, 37 cases were associated with AL amyloidosis, and 35% of patients had atrial fibrillation. The majority had an ischemic hemispheric stroke, and at least half involved a large artery [16]. Another study evaluated 15 patients with AL amyloidosis who were not receiving anticoagulation and were being considered for stem cell transplantation. Nine patients had arterial thromboembolic events: 3 had ischemic stroke, 2 had transient ischemic attacks, and 4 had other manifestations including peripheral arterial emboli and ocular and mesenteric ischemia. Out of these 9 patients, 7 had other associated risk factors [15].

Stroke has been reported to be particularly linked to arterial embolic events in patients with CA [13,14,16]. In a report of 54 autopsies, approximately 25% of patients had intracardiac thrombi [17]. In another study of 114 postmortem cases and 4 explanted hearts from patients with CA, thrombi were confirmed in 33% of specimens [18]. Feng et al identified intracardiac thrombi in 35% of patients with AL amyloidosis and CA [19]. Despite the high prevalence of intracardiac thrombi, published reports of ischemic stroke remain limited. Transthoracic echocardiography did not reveal intracardiac thrombi in our patient. However, this technique has been shown to have low sensitivity for detecting such thrombi in CA [14,19]. In our case, hemodynamic instability precluded transesophageal echocardiography. Brain MRI demonstrated an acute ischemic stroke in the middle cerebral artery with left internal carotid artery occlusion. Although these imaging findings suggested an artery-to-artery embolic mechanism, they did not establish the underlying thromboembolic source.

Interestingly, Zubkov et al reported carotid stenosis in only 3 patients with amyloidosis; 2 also had significant CA and recurrent ischemic stroke, leading the authors to favor a cardioembolic rather than a carotid mechanism [16]. Likewise, in our patient, advanced CA together with left internal carotid artery occlusion raised the possibility of both artery-to-artery embolism and cardioembolism, although the latter could not be excluded because transesophageal echocardiography was not feasible [19]. Therapeutic anticoagulation was therefore started based on careful assessment of thromboembolic and hemorrhagic risk. This decision also considered the recognized bleeding

This work is licensed under Creative Commons Attribution-NonCommercial-NoDerivatives 4.0 International (CC BY-NC-ND 4.0)

Indexed in: [PMC] [PubMed] [Emerging Sources Citation Index (ESCI)] [Web of Science by Clarivate]

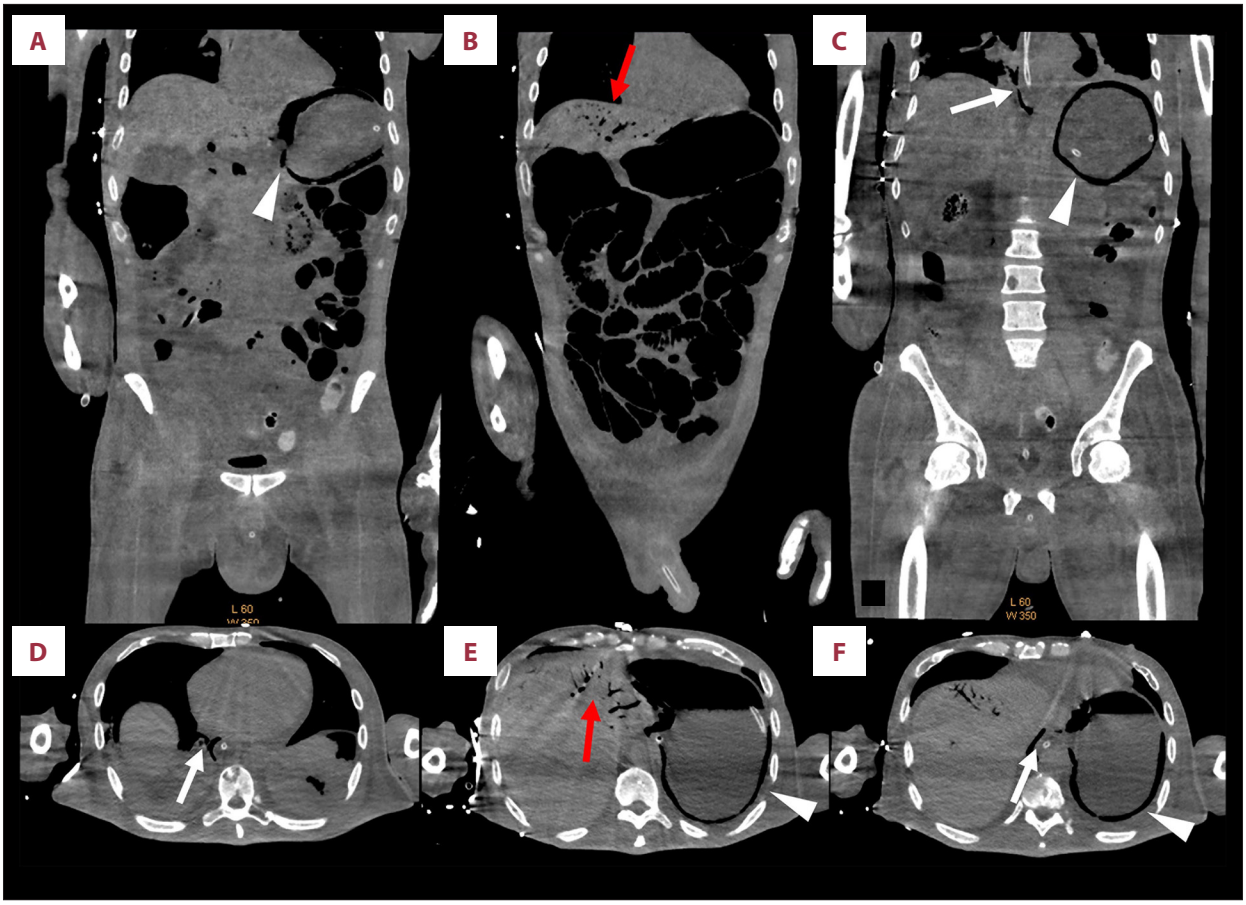


Figure 7. Abdominal computed tomography (CT) findings. Coronal CT images (**A-C**) demonstrate gastric pneumatosis (white arrowheads) in **A** and **C**, hepatic portal venous gas involving the portal vein and its left branch (red arrow) in **B**, and periesophageal gas consistent with pneumomediastinum (white arrows) in **C**. Axial CT images (**D-F**) demonstrate pneumomediastinum (white arrow) in **D**, gastric pneumatosis (white arrowheads) in **E** and **F**, hepatic portal venous gas involving the portal vein and its left branch (red arrow) in **E**, and periesophageal gas extending below the diaphragm into the upper abdomen (white arrow) in **F**.

tendency associated with AL amyloidosis due to vascular amyloid deposition and coagulation abnormalities [20]. Although antiplatelet therapy is generally recommended for secondary prevention of non-cardioembolic ischemic stroke [21], our patient's overall clinical context, including advanced CA, nephrotic-range proteinuria, plasma cell dyscrasia, left internal carotid artery occlusion, and the inability to exclude an intracardiac thrombus, raised persistent concern for an underlying cardioembolic source. Accordingly, anticoagulation was selected after multidisciplinary assessment despite the absence of definitive evidence establishing the stroke mechanism [22]. Intracardiac thrombi and cardioembolic events have been reported in patients with CA even in sinus rhythm, and available evidence supports individualized assessment of thromboembolic and bleeding risks when considering anticoagulation in this setting [22,23].

In a larger cohort of patients with CA (406 patients, including 134 with AL amyloidosis), the incidence of arterial thromboembolism was 7.6%. The majority of events were ischemic strokes (29 of 31), and 32% of strokes occurred in patients in sinus rhythm [24]. Several mechanisms have been proposed to explain arterial thromboembolism in AL amyloidosis and CA, including hypercoagulability, atrial mechanical dysfunction with intracardiac thrombus formation, endocardial injury, restrictive physiology leading to blood stasis, and valvular amyloid deposition [14,15,25,26]. In addition, MM is by itself associated with an increased risk of arterial thrombosis, including ischemic stroke, even before treatment [27]. Collectively, these observations suggest that systemic AL amyloidosis and MM create a multifactorial prothrombotic milieu that may predispose to both cardiac and extracardiac arterial embolism. Thromboembolic events are associated with poor prognosis in patients with CA [14,18,28]. Although the history of a fall prompted consideration of traumatic cervical arterial injury, CT angiography did not demonstrate findings suggestive of dissection. Nevertheless, the absence of arterial

APPROVED GALLEY PROOF

This work is licensed under Creative Commons Attribution-NonCommercial-NoDerivatives 4.0 International (CC BY-NC-ND 4.0)

Indexed in: [PMC] [PubMed] [Emerging Sources Citation Index (ESCI)] [Web of Science by Clarivate]

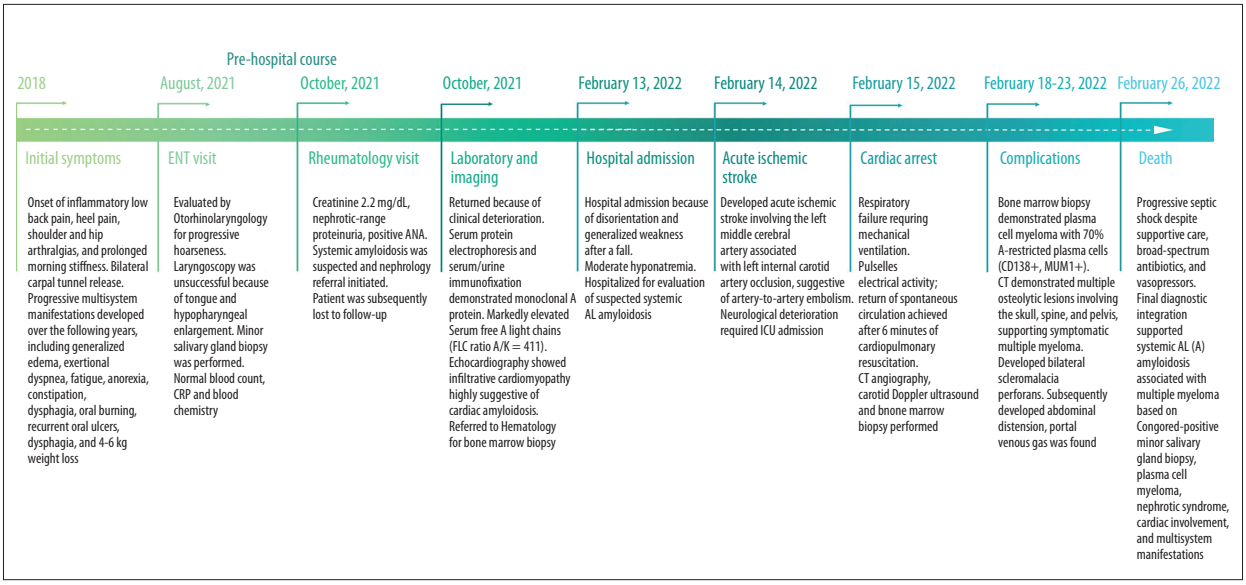


Figure 8. Timeline summarizing the chronological evolution of the major clinical findings and interventions, from initial symptom recognition to the fatal outcome. CRP, C-reactive protein; ENT, ears, nose, and throat; ANA, antinuclear antibodies; MCA, middle cerebral artery; CPR, cardiopulmonary resuscitation; AL, amyloid light chain; ICU, intensive care unit; CT, computed tomography.

APPROVED GALLEY PROOF

dissection did not establish the underlying thromboembolic mechanism, which remained uncertain.

Regarding ocular involvement, we did not identify any previous report of bilateral scleromalacia perforans occurring in patients with AL amyloidosis or MM. Ocular involvement in MM is uncommon and is most often reported in older patients. Nevertheless, it has also been described in younger individuals [29]. It usually affects orbital rather than intraocular structures and may result from plasma cell infiltration or hematologic complications [30,31]. To our knowledge, only 1 case of bilateral posterior scleritis has been reported in MM [32], whereas bilateral scleritis has been described in only 2 patients with AA amyloidosis, both associated with rheumatoid arthritis. In a series of patients with systemic AL amyloidosis, ocular manifestations occurred in 16% of patients and in 10% of those with AL amyloidosis associated with MM; however, scleritis was not observed in any patient [33]. Because the diagnosis of necrotizing scleritis requires careful evaluation of the underlying cause [34], the workup for the main causes—including connective tissue autoimmune diseases, ANCA-associated vasculitis, tuberculosis, and syphilis—was performed and results were negative. No additional infectious etiologies were clinically suspected based on the patient's ophthalmologic presentation. The pathogenesis of necrotizing scleritis has been linked to vasculitis mediated by immune complex deposition in autoimmune diseases [34]. An alternative or contributing mechanism may involve vascular compromise. In patients with necrotizing scleritis evaluated by fluorescein angiography, vaso-obliterative changes have been identified as a characteristic finding, including vascular stasis and partial venular occlusion, which if persistent, may progress to irreversible vascular closure [35]. Whether one or both of these mechanisms contributed to bilateral scleromalacia perforans in our patient remains uncertain. Tissue biopsy and immunofluorescence studies were not performed because of our patient's critical clinical condition. The diagnosis of scleromalacia perforans was established clinically by the ophthalmology team, consistent with current clinical practice, whereas ancillary imaging studies were considered complementary and not feasible during the patient's critical illness. Therefore, although bilateral scleromalacia perforans was clinically well established, its precise pathophysiological mechanism in our patient remains uncertain.

Gastrointestinal involvement is common. However, gastrointestinal perforation in particular remains as a rare although recognized complication. In a review of gastrointestinal perforation in patients with all types of amyloidosis, the authors found a total of 62 cases, 24 being in patients with AL amyloidosis in particular. Of the total number of perforations, 23 resulted in early death (10 with AL amyloidosis), and in 19 the information was not available. Regarding age group of the patients with AL amyloidosis and perforation, only 4 patients were under 50 years, including 2 women aged 39 and 43, and 2 men aged 23 and 46. All 4 had a small intestine perforation, and 3 died shortly after [36]. The 39-year-old patient had MM with end-stage renal failure requiring dialysis and died from postoperative complications [37]. The 43-year-old woman had renal, cardiac, and peripheral nerve involvement and died from a gastrointestinal perforation 4 days after a stem cell transplant

This work is licensed under Creative Commons Attribution-NonCommercial-NoDerivatives 4.0 International (CC BY-NC-ND 4.0)

Indexed in: [PMC] [PubMed] [Emerging Sources Citation Index (ESCI)] [Web of Science by Clarivate]

[38]. The youngest patient had renal and liver involvement. The 46-year-old patient survived but had no other organ involvement [36]. Most of the remaining patients with AL amyloidosis who died following intestinal perforation also had involvement of other organs, similar to our patient.

Regarding the subset of patients with AL amyloidosis with associated MM identified in this review (5 patients in total), 2 had early death. One had multisystem involvement, and in the other, this information was missing. Of the 3 surviving patients with MM, 2 had no other organ involvement and 1 had only renal involvement. Consistent with this review, our patient had advanced multisystem involvement, including CA, and subsequently experienced a rapidly fatal clinical course [36].

Histopathological studies have implicated amyloid deposition within the bowel wall and blood vessels, leading to tissue fragility and ischemic injury [37,39]. High-dose corticosteroid exposure has also been reported as a potential contributing factor in patients with MM [40]. In our patient, corticosteroid therapy was initiated for severe ocular involvement with sight-threatening potential rather than as disease-directed therapy for MM. Although corticosteroids may have represented a contributing factor, gastrointestinal perforation occurred in the setting of advanced multisystem AL amyloidosis and critical illness.

Several individual cases of gastrointestinal perforation associated with AL amyloidosis and MM have been reported [39,41]. Harada et al described a 75-year-old woman with a sigmoid perforation in whom histopathological examination demonstrated vascular wall thickening and stenosis attributed to AL amyloidosis associated with MM. In contrast to our patient, she had no advanced multisystem involvement or other life-threatening complications at the time of surgical intervention [39]. Fraser et al reported 2 cases of older women with duodenal perforation associated with AL amyloidosis and MM who were successfully managed conservatively [41]. Compared with these previously reported cases, our patient presented with simultaneous cardiac, neurologic, ocular, renal, and gastrointestinal involvement, representing a more complex clinical scenario.

Although gastrointestinal perforation is a life-threatening complication that requires consideration of surgical treatment, postoperative mortality in patients with gastrointestinal amyloidosis remains high (50-69%), largely due to severe organ involvement. It also depends on clinical context and surgical technique [39]. Our patient developed significant abdominal distention that progressed to hepatic portal venous gas. Although hepatic portal venous gas has traditionally been associated with bowel ischemia, necrosis, or perforation [42], benign and reversible causes have also been described. Reports of hepatic portal venous gas in the setting of amyloidosis remain exceptional. Yamamoto et al described a 63-year-old woman with rheumatoid arthritis-associated amyloidosis who presented with both hepatic portal venous gas and pneumatosis intestinalis, and was successfully managed conservatively, with complete radiologic resolution within 24 hours [43]. In contrast, our patient developed gastric pneumatosis, hepatic portal venous gas, pneumomediastinum with periesophageal gas extending below the diaphragm, peritoneal signs, and progressive hemodynamic deterioration, findings highly suggestive of upper gastrointestinal perforation. Histopathological confirmation of amyloid deposition within the affected gastrointestinal tissue was not obtained because surgical intervention was not performed. In addition, CT angiography could not be performed because of hemodynamic instability and worsening renal function. Autopsy was not performed because consent was declined by the family. Consequently, although ischemia has been proposed as a biologically plausible mechanism in previous reports, the precise pathophysiological mechanism underlying the gastrointestinal complication or its relationship to the patient's other severe complications could not be established with certainty.

It is important to distinguish what this case demonstrates directly from what remains speculative. Directly observed findings include Congo red-positive amyloid deposits, MM confirmed by bone marrow biopsy with λ light-chain restriction, nephrotic-range proteinuria, echocardiographic findings highly suggestive of CA, MRI-confirmed ischemic stroke, clinically diagnosed bilateral scleromalacia perforans, and CT findings of gastric pneumatosis, hepatic portal venous gas, and pneumomediastinum with periesophageal gas extending below the diaphragm. Together, these findings were highly suggestive of upper gastrointestinal perforation. Pathological confirmation of amyloid deposition within the affected cerebral, ocular, or gastrointestinal tissues was not available because surgical intervention was not performed, and permission for autopsy was declined by the family. Consequently, although ischemia has been proposed as a biologically plausible mechanism in previous reports, our case does not establish a causal pathophysiological link among these severe complications, and this hypothesis should be interpreted cautiously.

Thus, the novelty of this case does not lie in the individual complications but rather in the unusual convergence of 3 severe, life-threatening manifestations (ischemic stroke, bilateral scleromalacia perforans, and intestinal perforation) in a single middle-aged adult with AL amyloidosis associated with MM. Previous studies have shown that patients with AL amyloidosis associated with MM, particularly those with cardiac and multisystem involvement, have poorer outcomes [9,44]. Within this context, our case highlights the diagnostic challenges posed by advanced multisystem disease, and illustrates that severe, life-threatening complications may also occur in a middle-aged adult with AL amyloidosis associated with MM.

APPROVED GALLEY PROOF

This work is licensed under Creative Commons Attribution-NonCommercial-NoDerivatives 4.0 International (CC BY-NC-ND 4.0)

Indexed in: [PMC] [PubMed] [Emerging Sources Citation Index (ESCI)] [Web of Science by Clarivate]

APPROVED GALLEY PROOF

Conclusions

We present an unusual case of AL amyloidosis associated with MM in a middle-aged adult, in whom diagnostic delay was followed by simultaneous occurrence of ischemic stroke, bilateral scleromalacia perforans, and intestinal perforation—a combination not previously reported. The primary lesson of this case is diagnostic: amyloidosis and plasma cell disorders warrant strong consideration when nephrotic-range proteinuria and multisystem infiltrative features coexist, including younger adults. This single case serves as a clinical warning that delayed recognition may be followed by severe, potentially fatal complications.

Acknowledgements

We thank Adalberto Mosqueda, MSc, and Dr. Abraham Majluf-Cruz for their contributions to this case.

Department and Institution Where Work Was Done

Department of Internal Medicine, Hospital San Ángel Inn, Universidad, México City, México.

Informed Consent

Written informed consent for publication of the clinical case and images was obtained and signed by family member.

Declaration of Figures' Authenticity

All figures submitted have been created by the authors who confirm that the images are original with no duplication and have not been previously published in whole or in part.

References:

1. Gertz MA, Dispenzieri A. Systemic amyloidosis recognition, prognosis, and therapy. JAMA. 2020;324:79-89
2. Buxbaum JN, Dispenzieri A, Eisenberg DS, et al. Amyloid nomenclature 2022: Update, novel proteins, and recommendations by the International Society of Amyloidosis (ISA) Nomenclature Committee. Amyloid. 2022;29:213-19
3. Kumar N, Zhang NJ, Cherepanov D, et al. Global epidemiology of amyloid light-chain amyloidosis. Orphanet J Rare Dis. 2022;17:278
4. Staron A, Zheng L, Doros G, et al. Marked progress in AL amyloidosis survival: A 40-year longitudinal natural history study. Blood Cancer J. 2021;11:139
5. Muchtar E, Gertz MA, Kyle RA, et al. A modern primer on light chain amyloidosis in 592 patients with mass spectrometry–verified typing. Mayo Clin Proc. 2019;94:472-83
6. Kyle RA, Gertz MA. Primary systemic amyloidosis: Clinical and laboratory features in 474 cases. Semin Hematol. 1995;32:45-59
7. National Cancer Institute. SEER Cancer Stat Facts: Myeloma [Internet]. Bethesda, MD: National Cancer Institute; [cited 2026 Apr 23]. Available from: https://seer.cancer.gov/statfacts/html/mulmy.html
8. Kyle RA. Multiple myeloma: Review of 869 cases. Mayo Clin Proc. 1975;50:29-40
9. Vela-Ojeda J, García-Ruiz Esparza MA, Padilla-González Y, et al. Multiple myeloma-associated amyloidosis is an independent high-risk prognostic factor. Ann Hematol. 2009;88:59-66
10. Kumar S, Dispenzieri A, Lacy MQ, et al. Revised prognostic staging system for light chain amyloidosis incorporating cardiac biomarkers and serum free light chain measurements. J Clin Oncol. 2012;30:989-95
11. McCluskey P, Wakefield D. Intravenous pulse methylprednisolone in scleritis. Arch Ophthalmol. 1987;105:793-97
12. Jabs DA, Mudun A, Dunn JP, Marsh MJ. Episcleritis and scleritis: Clinical features and treatment results. Am J Ophthalmol. 2000;130:469-76
13. Dixit A. Acute ischemic stroke as initial manifestation of cardiac amyloidosis. Neurol Sci. 2024;45:4615-16
14. Zhang X, Liu Y, Yan X, et al. Cerebral embolism secondary to cardiac amyloidosis: A case report and literature review. Exp Ther Med. 2017;14:6077-83
15. Hausfater P, Costedoat-Chalumeau N, Amoura Z, et al. AL cardiac amyloidosis and arterial thromboembolic events. Scand J Rheumatol. 2005;34:315-19
16. Zubkov AY, Rabinstein AA, Dispenzieri A, Wijdicks EFM. Primary systemic amyloidosis with ischemic stroke as a presenting complication. Neurology. 2007;69:1136-41
17. Roberts WC, Waller BF. Cardiac amyloidosis causing cardiac dysfunction: Analysis of 54 necropsy patients. Am J Cardiol. 1983;52:137-46
18. Feng D, Edwards WD, Oh JK, et al. Intracardiac thrombosis and embolism in patients with cardiac amyloidosis. Circulation. 2007;116:2420-26
19. Feng D, Syed IS, Martinez M, et al. Intracardiac thrombosis and anticoagulation therapy in cardiac amyloidosis. Circulation. 2009;119:2490-97
20. Mumford AD, O'donnell J, Gillmore JD, et al. Bleeding symptoms and coagulation abnormalities in 337 patients with AL-amyloidosis. Br J Haematol. 2000;110:454-60
21. Kleindorfer DO, Towfighi A, Chaturvedi S, et al. 2021 Guideline for the prevention of stroke in patients with stroke and transient ischemic attack: A guideline from the American Heart Association/American Stroke Association. Stroke. 2021;52:e364-e467
22. Nicol M, Siguret V, Vergaro G, et al. Thromboembolism and bleeding in systemic amyloidosis: A review. ESC Heart Fail. 2022;9:11-20
23. Giancaterino S, Urey MA, Darden D, Hsu JC. Management of arrhythmias in cardiac amyloidosis. JACC Clin Electrophysiol. 2020;6:351-61
24. Cappelli F, Tini G, Russo D, et al. Arterial thromboembolic events in cardiac amyloidosis: A look beyond atrial fibrillation. Amyloid. 2021;28:12-18
25. Suleiman S, Coughlan JJ, Moore D. Cardiac amyloidosis presenting with recurrent ischaemic strokes. BMJ Case Rep. 2020;13:e231910
26. Gamba G, Montani N, Anesi E, et al. Abnormalities in thrombin-antithrombin pathway in AL amyloidosis. Amyloid. 1999;6:273-77
27. Kristinsson SY, Pfeiffer RM, Björkholm M, et al. Arterial and venous thrombosis in monoclonal gammopathy of undetermined significance and multiple myeloma: A population-based study. Blood. 2010;115:4991-98
28. Halligan CS, Lacy MQ, Vincent Rajkumar S, et al. Natural history of thromboembolism in AL amyloidosis. Amyloid. 2006;13:31-36
29. Omoti AE, Omoti CE. Review article: Ophthalmic manifestations of multiple myeloma. West Afr J Med. 2007;26:265-68
30. Bouazza M, Youssefi H, Bouanani N. Ocular manifestations in hematological disorders. Cureus. 2022;14:e27941
31. Ashton N. Ocular changes in multiple myelomatosis. Arch Ophthalmol. 1965;73:487-94
32. Güngör SG, Akkoyun İ, Çoban-Karataş M, Karakuş S. Bilateral posterior scleritis in a case with multiple myeloma. Turk J Oftalmol. 2014;44:481-83
33. Dammacco R, Merlini G, Lisch W, et al. Amyloidosis and ocular involvement: An overview. Semin Ophthalmol. 2020;35:7-26
34. Dutta Majumder P, Agarwal S, Shah M, et al. Necrotizing scleritis: A review. Ocul Immunol Inflamm. 2024;32:1405-19
35. Watson PG, Bovey E. Anterior segment fluorescein angiography in the diagnosis of scleral inflammation. Ophthalmology. 1985;92:1-11

This work is licensed under Creative Commons Attribution-NonCommercial-NoDerivatives 4.0 International (CC BY-NC-ND 4.0)

Indexed in: [PMC] [PubMed] [Emerging Sources Citation Index (ESCI)] [Web of Science by Clarivate]

36. Shaulov A, Avivi I, Cohen Y, et al. Gastrointestinal perforation in light chain amyloidosis in the era of novel agent therapy – A case series and review of the literature. Amyloid. 2018;25:11-17
37. Ng SB. Rare presentation of intestinal amyloidosis with acute intestinal pseudo-obstruction and perforation. J Clin Pathol. 2002;55:876
38. Schulenburg A, Kalhs P, Oberhuber G, et al. Gastrointestinal perforation early after peripheral blood stem cell transplantation for AL amyloidosis. Bone Marrow Transplant. 1998;22:293-95
39. Harada K, Ichikawa D, Konishi H, et al. Perforation of the sigmoid colon and massive ischemia of the small intestine caused by amyloidosis associated with multiple myeloma: A case report. Int Surg. 2014;99:685-90
40. Vaxman I, Al Saleh AS, Kumar S, et al. Colon perforation in multiple myeloma patients – A complication of high-dose steroid treatment. Cancer Med. 2020;9:8895-901
41. Fraser AG, Nicholson GI. Duodenal perforation in primary systemic amyloidosis. Gut. 1992;33:997-99
42. Liebman PR, Patten MT, Manny J, et al. Hepatic-portal venous gas in adults. Ann Surg. 1978;187:281-87
43. Yamamoto A, Kawahito Y, Niimi M, et al. Pneumatosis intestinalis and hepatic portal venous gas caused by gastrointestinal perforation with amyloidosis. J Clin Gastroenterol. 2008;42:758-59
44. Madan S, Dispenzieri A, Lacy MQ, et al. clinical features and treatment response of light chain (AL) amyloidosis diagnosed in patients with previous diagnosis of multiple myeloma. Mayo Clin Proc. 2010;85:232-38

APPROVED GALLEY PROOF

This work is licensed under Creative Commons Attribution-NonCommercial-NoDerivatives 4.0 International (CC BY-NC-ND 4.0)

Indexed in: [PMC] [PubMed] [Emerging Sources Citation Index (ESCI)] [Web of Science by Clarivate]